Physical Layer Network Coding with Gaussian Waveforms using Soft Interference Cancellation

Matthias Woltering, Dirk Wübben, and Armin Dekorsy
Department of Communications Engineering
University of Bremen, Bremen, Germany
Email: {woltering, wuebben, dekorsy}@ant.uni-bremen.de

Abstract—**The performance of physical-layer network coding (PLNC) in two way relay channels (TWRCs) is significantly decreased by impairments like carrier frequency offsets or timing offsets. This mismatch cannot be completely compensated at the receiver side, even if the offsets are known. Multi-carrier systems with Gaussian waveforms for TWRC systems are more robust against the impact of these offsets. In comparison to rectangular multi-carrier systems, Gaussian waveforms have a better time-frequency shape and they provide improved spectral efficiency due to lower out of band radiations. In this paper, we introduce a multi-carrier TWRC system with Gaussian waveforms and develop an adapted soft interference cancellation (SIC) equalizer to consider the intrinsic interference of the Gaussian transmit/receive filters. The presented results show, that systems with Gaussian waveforms achieve bit error rates close to the rectangular waveforms in PLNC systems while being more robust against Doppler and delay spreads.**

I. Introduction

A rapid expansion from single user transmission to networks supporting a huge number of services has been developed in the last decades. Main challenges are the high transmission rates at low costs. A key technology for future mobile communication systems is the principle of cooperative communication. The enhancement of coverage for applications with given quality of service (QoS) constraints is one advantage of this scheme [1]–[4]. By using assisting relay stations between users, the path losses of the transmission links can be significant reduced. Allowing transmissions of two users simultaneously to an assisting relay in a so-called multiple access (MA) phase using a two way relay channel (TWRC) achieves further improvement of the spectral efficiency. This idea of physical-layer network coding (PLNC) in TWRCs was introduced in [4]–[8]. This transmission results in the superposition of the signals of both users at the relay. Based on this received signal, the relay constructs a relay message, which uses PLNC and it is transmitted to both users in the broadcast (BC) phase. The users can obtain the message of the other user by simply subtracting their own message transmitted previously.

Many recent transmission schemes like WLAN, LTE or DVB-T are using orthogonal frequency division multiplexing (OFDM) as multi-carrier scheme, utilizing rectangular transmit and receive filters per sub-carrier. Correspondingly, the application of OFDM for PLNC has been introduced and analyzed in [8]–[14]. Rectangular waveforms are orthogonal in the frequency domain, but at the cost of a broad spectral shape. Additionally, they come with a high sensitivity against offsets. Hence, carrier frequency offsets (CFOs) have a severe influence in the performance of OFDM systems, which are in particular also the case for PLNC systems [15], [16]. However, the impact of impairments like CFO, timing offset (TO) and other channel influences can be reduced significantly by applying other waveforms [17].

In this paper, we combine the robustness of a Gaussian waveform with a better time-frequency localization property in generalized frequency division multiplexing (GFDM) [18]–[20]. The higher robustness comes at the expense of additional intrinsic interference introduced by transmit filters that does not fulfill the first Nyquist criterion. Here, we applying a two step approach by firstly treating the additional interference by an equalizer, where secondly the superposition of the two users can be exploited in PLNC detection algorithms. We propose in this paper the combination of an additional soft interference cancellation (SIC) processing block and PLNC detection at the relay, iteratively. The bit error rate (BER) performance of multi-carrier schemes is compared regarding the iterative equalizer for handling extrinsic and intrinsic interference introduced by the channel and corresponding waveforms. Furthermore, the multi-carrier transmission scheme cyclic prefix OFDM (CP-OFDM) with a low complexity one-tap equalizer is used as a benchmark scheme as it is the common SotA transmission scheme.

The paper is organized as follows: In Section II, the overall transmission scheme based on TWRC in the MA phase is introduced. Section III describes the procedures at the relay. First, the PLNC detection schemes are introduced and further the equalizing with and without an iterative structure is shown. Furthermore, in Section IV simulation results for different channel realizations and offsets are given and also the robustness of the Gaussian waveform in TWRC is presented. Section V concludes the paper.

II. System model

Let $\mathbf{u}_\mathrm{A}$ and $\mathbf{u}_\mathrm{B}$ be two binary sequences of length N_u which are encoded by a linear encoder $\mathcal{C}$ to sequences $\mathbf{c}_\mathrm{A} \in \mathbb{F}^{N_\mathrm{c}}$ and $\mathbf{c}_\mathrm{B} \in \mathbb{F}^{N_\mathrm{c}}$. The modulator $\mathcal{M}$ maps $\log_2(M)$ code bits to one M-ary symbol $d_i^{(k,\ell)}$ for each user $i \in \{\mathrm{A}, \mathrm{B}\}$ in the matrix $\mathbf{D}_i$ of size $\in \mathbb{C}^{N_k \times N_\ell}$ with N_k sub-carriers and N_ℓ symbols used in one transmission frame. Each symbol $d_i^{(k,\ell)}$ corresponds to a symbol transmitted on sub-carrier kF at time instance ℓT with the symbol spacing F in frequency and symbol spacing T in time domain. Fig. 1 shows the system

978-1-4799-8088-8/15/$31.00 ©2015 IEEE

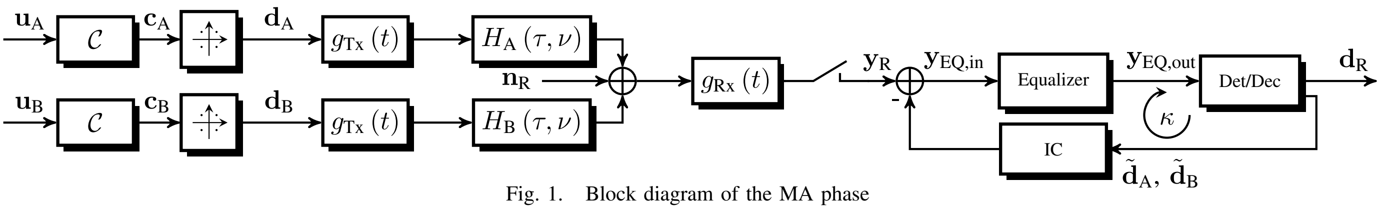

Fig. 1. Block diagram of the MA phase

model. We assume that both users equipped with one antenna transmit their messages $\mathbf{d}_{\mathrm{A}}$ and $\mathbf{d}_{\mathrm{B}}$ simultaneously on the same resources to the relay also equipped with one antenna in the MA-phase. As both signals are superimposed through individual channels the received signal $\mathbf{y}_{\mathrm{R}}$ is given by

$$\begin{aligned}\mathbf{y}_{\mathrm{R}} &= \mathbf{V}_{\mathrm{A}} \cdot \mathbf{d}_{\mathrm{A}} + \mathbf{V}_{\mathrm{B}} \cdot \mathbf{d}_{\mathrm{B}} + \mathbf{n}_{\mathrm{R}} \\ &= \left(\mathbf{\Lambda}_{\mathrm{A}} + \overline{\mathbf{\Lambda}}_{\mathrm{A}}\right) \cdot \mathbf{d}_{\mathrm{A}} + \left(\mathbf{\Lambda}_{\mathrm{B}} + \overline{\mathbf{\Lambda}}_{\mathrm{B}}\right) \cdot \mathbf{d}_{\mathrm{B}} + \mathbf{n}_{\mathrm{R}} \ , \qquad (1)\end{aligned}$$

where the symbol vector $\mathbf{d}_i = \mathrm{vec}\{\mathbf{D}_i\}$ of size $N_k N_\ell$ with $i \in \{\mathrm{A}, \mathrm{B}\}$ is a stacked version of matrix $\mathbf{D}_i$ using the vec $\{\cdot\}$ operator. In (1) the matrix $\mathbf{V}_i \in \mathbb{C}^{N_k N_\ell \times N_k N_\ell}$ is the effective channel matrix of user i combining two effects [21]:

- *Channel Influence:* All influences of the channel, like channel gain $h_\mu^{(i)}$ of path μ, Doppler spread $\nu_\mu^{(i)}$, CFO $\Delta\nu^{(i)}$ delay spread, $\tau_\mu^{(i)}$ and TO $\Delta\tau^{(i)}$ can be given by the delay-Doppler function:

$$\begin{aligned}H_i(\tau,\nu) = &\sum_{\mu=0}^{N_{\mathrm{h}}-1} h_\mu^{(i)} \delta\left(t - \tau_\mu^{(i)} - \Delta\tau^{(i)}\right) \\ &\cdot \delta\left(\nu - \nu_\mu^{(i)} - \Delta\nu^{(i)}\right) \quad , \qquad (2)\end{aligned}$$

  where N_{h} gives the number of channel taps and $\delta(\cdot)$ is the Dirac delta function.
- *Transmit & receive filter:* The second influence is the impact of the transmit $g_{\mathrm{Tx}}(t)$ and receive filter $g_{\mathrm{Rx}}(t)$, calculated with the ambiguity function and given in [21].

Every element in the effective channel matrix in $\mathbf{V}_i$ gives the influences of a symbol $d_i^{(k,\ell)}$ on the transmit time-frequency point (k,ℓ) to a receive signal $y_{\mathrm{R}}^{(k',\ell')}$ at receive time-frequency point (k',ℓ'). A detailed description of $\mathbf{V}_i$ is given in [16], [21]. Each matrix $\mathbf{V}_i$ can be separated in a diagonal part $\mathbf{\Lambda}_i$, describing the influence on the desired signal and an off-diagonal part $\overline{\mathbf{\Lambda}}_i$, characterizing the inter-symbol interference (ISI) and inter-carrier interference (ICI) introduced by the self-interference of the filters and the influence of the channel.

Fig. 2 illustrates exemplary amplitudes of matrix $\mathbf{V}_i$ for a rectangular and a Gaussian waveform with a flat fading channel and without and with presence of a CFO $\Delta\nu^{(i)} = 0.2F$ showing $N_k = 7$ sub-carriers and $N_\ell = 7$ time symbols in a frame. If no CFO is present the rectangular has a perfect diagonal structure, which means no interference is introduced, whereas the Gaussian waveform introduces self-interference. By presence of CFO the rectangular waveform experience a higher influence in comparison to the Gaussian waveform, i.e., the rectangular waveform is more sensitive to offsets than its Gaussian counterpart.

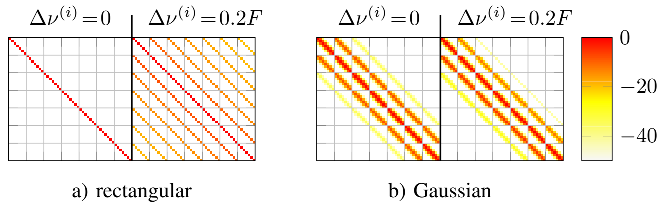

Fig. 2. Matrices $\mathbf{V}_i$ for a) rectangular waveform and b) Gaussian waveform. Flat fading channel with and without influence of additional CFO.

III. Relay processing

As described in Section II using non-orthogonal waveforms will introduce additional interference within a GFDM transmission. However, with wireless channels, receivers always have to deal with channel influences like delay spread or Doppler spread. Especially CFOs of two different users in TWRC introduce a severe degradation in the performance as they can not be resolved separately due to the superimposed received signal. For that, the receiver is faced with interference and thus an equalizer is always required, which deals with the interference from the channel as well as the interference coming from the waveforms. While the PLNC detector [8] will exploit the superposition of the two users, the equalizer is designed such that the output provides signals which are well suited for these detection schemes.

A. PLNC Detection Schemes

Based on the equalizer output $\mathbf{y}_{\mathrm{EQ,out}}$ in Fig. 1 the a-posteriori probabilitys (APPs) are calculated and further processed by corresponding PLNC detection schemes [5], [7], [8].

- *Separate Channel Decoding (SCD):* The SCD scheme estimates the source codeword $\mathbf{c}_i$ of each user separately based on the L-values per code bit of each user using the APPs and generates the relay codeword $\hat{\mathbf{c}}_{\mathrm{R}} = \hat{\mathbf{c}}_{\mathrm{A}} \oplus \hat{\mathbf{c}}_{\mathrm{B}}$ afterwards.
- *Generalized-Joint Channel Decoding and Physical-Layer Network Coding (G-JCNC):* The G-JCNC scheme developed in [7], [8] directly feeds the APPs to a non-binary decoder which fully exploits the gains of both channel codes jointly. The estimate of the non-binary joint codeword $\hat{\mathbf{c}}_{\mathrm{AB}} \in \mathbb{F}_2^2$ is finally used to estimate the relay codeword $\hat{\mathbf{c}}_{\mathrm{R}}$.

In addition to the estimation of the relay codeword, both schemes provide also soft estimates of the source codewords $\tilde{\mathbf{c}}_{\mathrm{A}}$ and $\tilde{\mathbf{c}}_{\mathrm{A}}$. By omitting the indices's for (k,ℓ) and (k',ℓ') with the BPSK mapping $d_i = 1 - 2c_i$ the soft symbols $\tilde{d}_i$ for SCD can be calculated by [22]

$$\tilde{d}_i = \tanh\left(L(c_i)/2\right) \quad . \qquad (3)$$

Here, $L(c_i)$ is the log-likelihood ratio (LLR) value of code bit c_i. The soft symbols for the G-JCNC are calculated based on the APPs $P_{c_\mathrm{A},c_\mathrm{B}} = \Pr\{(c_\mathrm{A}, c_\mathrm{B})|y_\mathrm{R}\}$ at the output of the decoder [16]:

$$\begin{aligned}\tilde{d}_\mathrm{A} &= \tanh\left(\log\left(\left(P_{0,0} + P_{0,1}\right) / \left(P_{1,0} + P_{1,1}\right)\right)\right)\\ \tilde{d}_\mathrm{B} &= \tanh\left(\log\left(\left(P_{0,0} + P_{1,0}\right) / \left(P_{0,1} + P_{1,1}\right)\right)\right) \quad . \end{aligned} \qquad (4)$$

Note that this can be simply extended to higher modulation schemes. The property of providing soft symbols for each codeword of both users is essential for iterative detection of TWRC systems [16]. Thus, the popular joint channel decoding and physical-layer network coding (JCNC) scheme, which directly estimated the relay codeword without providing estimates for the source codewords, is omitted here [4].

B. Linear Equalizer

In order to suppress interference from other time-frequency points and keeping the superposition of both users, we designed in [23] a linear equalizer following the minimum mean square error (MMSE) criterion. The equalizer only takes the dominant neighboring terms into account but ignores interference from other time-frequency components. To reduce the complexity, we focus on an equalizer which only uses the direct adjacent neighbors in the time-frequency grid [23].

C. Soft Interference Cancellation

Using now the estimated symbols, we can calculate the interference added by the other data symbols and subtract this from receive signal $\mathbf{y}_\mathrm{R}$, which will be fed to the equalizer, as shown in the right part of Fig. 1. This will further improve the estimation performance [22], iteratively. Thus, in iteration κ the equalizer input signal is given by

$$\mathbf{y}_\mathrm{EQ,in}^{(\kappa)} = \mathbf{y}_\mathrm{R} - (\overline{\mathbf{\Lambda}}_\mathrm{A} \cdot \tilde{\mathbf{d}}_\mathrm{A}^{(\kappa-1)} + \overline{\mathbf{\Lambda}}_\mathrm{B} \cdot \tilde{\mathbf{d}}_\mathrm{B}^{(\kappa-1)}) \quad , \qquad (5)$$

where $\tilde{\mathbf{d}}_\mathrm{A}^{(\kappa-1)}$ and $\tilde{\mathbf{d}}_\mathrm{B}^{(\kappa-1)}$ denote the estimates for the transmit signals achieved in the previous iteration by the common PLNC detector. Note that for the first iteration the symbols $\tilde{\mathbf{d}}_i^{(0)} = 0$ are initialized yielding the trivial linear equalizer of [23]. In higher iterations, the equalizer will be calculated based on the effective channel matrix $\mathbf{V}_i - \overline{\mathbf{\Lambda}}_i$, due to the reduction of the interference of the SIC. After N_κ iterations the detector provides the estimated relay codeword $\hat{\mathbf{c}}_\mathrm{R}$, which is mapped to the relay symbol vector $\mathbf{d}_\mathrm{R}$.

IV. Performance analysis

For the performance evaluation a multi-carrier system with BPSK modulation is considered where Rayleigh fading channels with N_h complex channel coefficient $h_\mu^{(i)}$ are assumed for each user $i \in \{\mathrm{A}, \mathrm{B}\}$. The time delay $\tau_\mu^{(i)}$ and the Doppler shift $\nu_\mu^{(i)}$ of channel tap μ are equally distributed within τ_max and ν_max, respectively. In total, $N_k = 32$ sub-carriers and $N_\ell = 10$ time symbols are used to generate a frame containing 320 data symbols.

Here we will compare two different multi-carrier transmission schemes:

- *CP-OFDM:* We focus on CP-OFDM implementing CP lengths of $T_\mathrm{CP} \approx 10\%T$, $20\%T$ and $30\%T$ and a simple **one-tap equalizer** per sub-carrier in the frequency domain.
- *GFDM:* In contrast to the simple equalizer structure in CD-OFDM, here GFDM will always use the **iterative structure** in (5). In this multi-carrier transmission, we focus on the Gaussian waveform.
- *Plain OFDM:* Additionally, we consider **plain OFDM** without any CP using a simple **one-tap equalizer** and the **iterative SIC** structure.

To analyze the performance, we focus on BER measurements in the MA phase at the relay, because this is the bottleneck of the transmission.

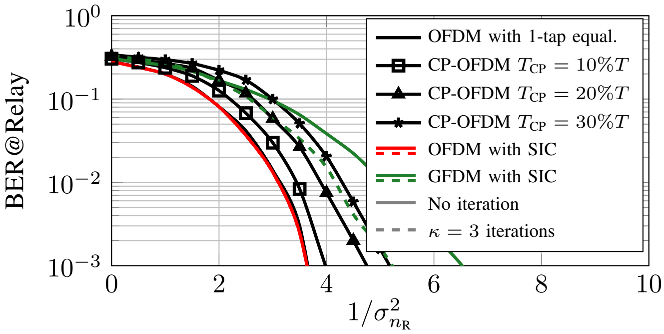

Fig. 3. Frequency flat channel, no delay spread $\tau_\mathrm{max} = 0$, no Doppler spread $\nu_\mathrm{max} = 0$, $\Delta\nu_\mathrm{A} = 0$ and $\Delta\nu_\mathrm{B} = 0$, PLNC detection scheme: G-JCNC

In Fig. 3 the multi-carrier schemes are compared in a frequency flat fading one tap channel $N_\mathrm{h} = 1$, showing only the influences of the waveforms regarding the detection scheme G-JCNC. Thus, $\overline{\mathbf{\Lambda}}_i$ has only zero elements in case of the rectangular shape, whereas the Gaussian waveform will have interference terms $\overline{\mathbf{\Lambda}}_i \neq \mathbf{0}$. As expected, the best performance is achieved by the orthogonal schemes OFDM with no CP, because the channel introduces no ISI/ICI and a simple one-tap equalizer is sufficient to equalize the channel impact. Larger CPs lead to an SNR loss $\gamma_\mathrm{CP} = 10\log_{10}\left(T/(T + T_\mathrm{CP})\right)$ in efficiency in comparison to the plain OFDM, which are $\gamma_\mathrm{CP} = -0.389\mathrm{dB}, -0.746\mathrm{dB}$ and $-1.1810\mathrm{dB}$ for the corresponding CP length. The OFDM with SIC also achieves the same performance, but at higher costs, due to an increased complexity of the larger equalizer. Applying iterations can not gain in performance, because no interference was introduced by the channel. The GFDM scheme with Gaussian waveform has a slightly worse performance due to the additional interference. By utilizing the SIC structure the performance is improved and it is similar to the CP-OFDM with a CP of length 30%.

Fig. 4 shows the performance in a frequency selective channel ($\tau_\mathrm{max} = 0.2T$) introducing ISI. The plain OFDM with 1-tap equalizer has a severe degradation due to the impact of ISI. This interference will not be taken into account in the equalizer process. The CP-OFDM with CP length of 20% can deal with this interference, because the maximum delay does not exceed the CP length. For a CP of 30% and 10% the performance is slightly worse, due to the SNR loss of the

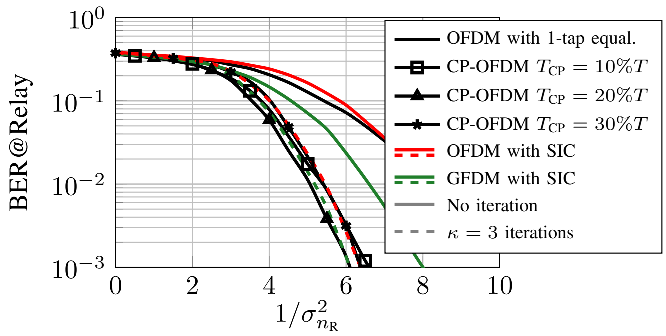

Fig. 4. Channel with delay spread $\tau_{\max} = 0.2T$ and Doppler spread $\nu_{\max} = 0$, no CFO $\Delta\nu^{(A)} = 0$ and $\Delta\nu^{(B)} = 0$.

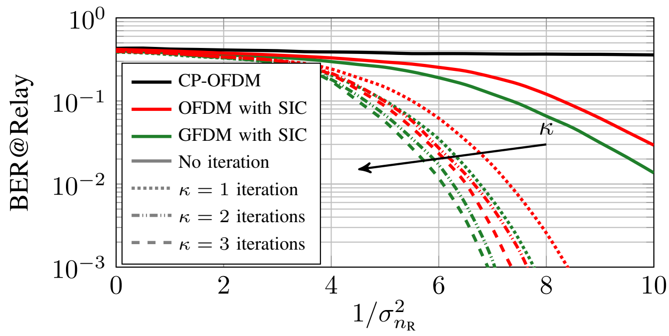

Fig. 6. Iterations analysis in channels with high additional CFOs of $\Delta\nu_A = 0.2F$ and $\Delta\nu_B = -0.2F$. $\tau_{\max} = 0.2T$ and $\nu_{\max} = 0$

guard interval and the violation the CP length, respectively. The GFDM schemes will achieve approximately the same performance by using the iterative structure. In the sequel, we will always use the CP-OFDM with a guard interval of 20% as benchmark. Further we skip here the OFDM with 1-tab equalizer, due to the huge performance degradation

In contrast to the previous scenario, Fig. 5 shows the performance with additional CFOs $\Delta\nu^{(A)} = 0.1F$ and $\Delta\nu^{(B)} = -0.1F$ with both PLNC detection schemes. As stated in [16], [24] an average CFO compensation is always possible and will achieve the best BER performance. Therefore, we only focus on symmetric CFOs, i.e., $\left|\Delta\nu^{(A)}\right| = \left|\Delta\nu^{(B)}\right|$. The CFOs cause a huge performance loss in the BER performance of CP-OFDM even by applying a large CP. In contrast to that, the GFDM schemes with an iterative structure outperform all other schemes. In this figure the performance results of the SCD are also shown. The G-JCNC outperforms the SCD by approx. 1dB due to exploiting the full channel coding gain at the detection process.

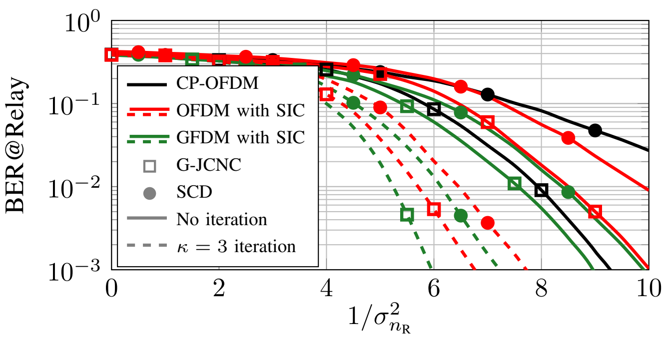

Fig. 5. Impact of BER performance with additional CFOs $\Delta\nu^{(A)} = 0.1F$ and $\Delta\nu^{(B)} = -0.1F$ and G-JCNC and SCD, $\tau_{\max} = 0.2T$ and $\nu_{\max} = 0$

In Fig. 6 we focus on the performance by a further increased difference of the CFOs regarding different numbers of iterations. In this scenario, the BER performance of CP-OFDM totally fails, whereas the OFDM with SIC outperforms CP-OFDM. The largest gain by iteration is achieved after the first iteration. Further iterations will only achieve a slightly better performance. The Gaussian waveform outperforms the scheme using OFDM with SIC.

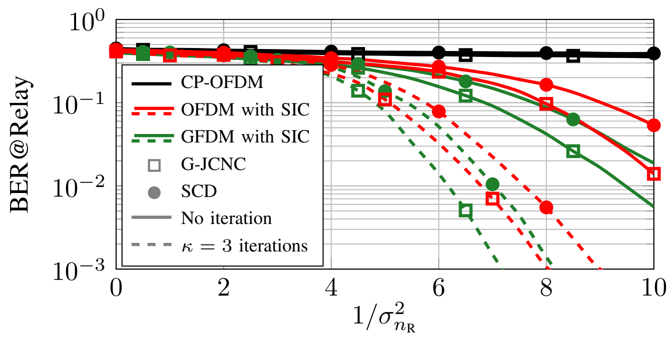

Fig. 7. Influences of Doppler and delay spread. $\tau_{\max} = 0.2T$ and $\nu_{\max} = \pm 0.2F$ with no additional CFO $\Delta\nu^{(A)} = 0$ and $\Delta\nu^{(B)} = 0$.

The channel parameters for Fig. 7 include a general Doppler spread of maximum $\nu_{\max} = \pm 0.2F$ and a delay spread of $\tau_{\max} = 0.2T$. Here, no additional CFOs are assumed. In this scenario, the CP-OFDM also totally fails in BER performance at the relay. We can observe that GFDM is more robust against spreading in time and frequency.

The robustness against different delay $\tau_{\max}$ and Doppler spreads $\nu_{\max}$ are shown in Fig. 8 regarding the G-JCNC scheme. Here the BER performance at a middle region with a fixed noise variance of $1/\sigma^2_{n_R} = 5$dB is considered. For plain OFDM in Fig. 7(a) with a one-tap equalizer the performance is highly sensitive against offsets in time and frequency direction. Fig. 7(b) shows the improvement by using a CP (here 30%), which increases the robustness against ISI. The system is clearly more robust against time spreads, but if the time spread exceeds the CP, the system will have huge degradations in the BER performance, due to the simple equalizer structure. The improvement by an iterative equalizer in OFDM is illustrated in Fig. 7(c). This scheme is more robust against delays spreads, but has a severe influence with the presence of Doppler shifts, due to the large spreading of the rectangular filter in the frequency domain. GFDM applying Gaussian waveforms with good localization properties is given in 7(d), it is more robust with both spreads in time and frequency direction. This could be expected due to the isotropic property of the Gaussian waveform. Thus, GFDM with Gaussian waveforms is well suited for TWRC using PLNC and outperforms the other schemes under practical constraints.

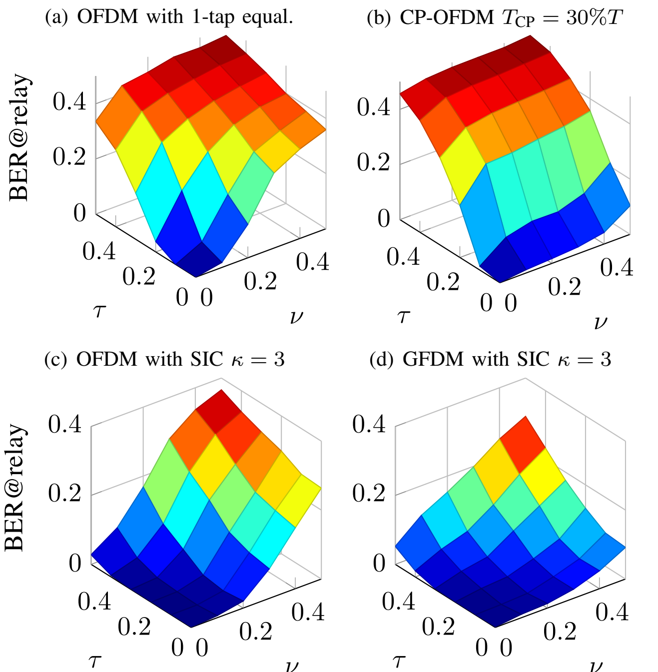

Fig. 8. BER performance at the relay with noise variance $1/\sigma^2_{n_R} = 5$dB with different $\tau_{\max}$ and $\nu_{\max}$.

V. Conclusion

In this paper we applied general multi-carrier systems for TWRC systems to reduce the impact of time and frequency impairments. In order to reduce the remaining interference after linear equalization, we developed an iterative TWRC detection scheme. Considering impairments and channel impacts the performance of the GFDM is more robust against these impacts by using an equalizer which only takes adjacent neighbors in the time-frequency grid into account, yielding a low complexity equalizer. Furthermore, the performance is highly improved by canceling interference in an iterative structure.

VI. Acknowledgment

This work was supported in part by the German Research Foundation (DFG) under grant WU 499/10-1 within the priority program “Communication in Interference Limited Networks (COIN)”, SPP 1397.

References

[1] F.-H.P. Fitzek, M. V. Pedersen, J. Heide, and M. Médard, “Network Coding: Applications and Implementations on Mobile Devices,” in *5th ACM Workshop on Performance Monitoring and Measurement of Heterogeneous Wireless and Wired Networks (PM2HW2N ’10)*, New York, NY, USA, 2010, ACM.

[2] M. Dohler and Y. Li, *Cooperative Communications: Hardware, Channel & PHY*, Wiley, Chichester, U.K., 2010.

[3] R. Pabst, B. H. Walke, D.C. Schultz, P. Herhold, H. Yanikomeroglu, S. Mukherjee, H. Viswanathan, M. Lott, W. Zirwas, M. Dohler, H. Aghvami, D.D. Falconer, and G.P. Fettweis, “Relay-based Deployment Concepts for Wireless and Mobile Broadband Radio,” *IEEE Communications Magazine*, vol. 42, no. 9, pp. 80–89, Sept 2004.

[4] S. Zhang, S.C. Liew, and P.P. Lam, “Hot Topic: Physical-layer Network Coding,” in *12th annual International Conference on Mobile Computing and Networking (MobiCom 06)*, Los Angeles, CA, USA, 2006.

[5] S. Zhang, S.C. Liew, and P.P. Lam, “On the Synchronization of Physical-Layer Network Coding,” in *IEEE Information Theory Workshop (ITW ’06)*, Chengdu, China, Oct 2006, pp. 404–408.

[6] P. Popovski and H. Yomo, “Physical Network Coding in Two-Way Wireless Relay Channels,” in *IEEE International Conference on Communications (ICC’ 07)*, Glasgow, GB, June 2007.

[7] D. Wübben and Y. Lang, “Generalized Sum-Product Algorithm for Joint Channel Decoding and Physical-Layer Network Coding in Two-Way Relay Systems,” in *2010 IEEE Global Telecommunications Conference GLOBECOM 2010*, Miami, Fl, USA, Dec. 2010, IEEE.

[8] D. Wübben, “Joint Channel Decoding and Physical-Layer Network Coding in Two-Way QPSK Relay Systems by a Generalized Sum-Product Algorithm,” in *Communication Systems (ISWCS), 2010 7th*, York, Great Britain, Sept. 2010.

[9] B. Han, W. Wang, and M. Peng, “Optimal Resource Allocation for Network Coding in Multiple Two-Way Relay OFDM Systems,” in *IEEE Wireless Communications and Networking Conference (WCNC 12)*, Paris, France, April 2012.

[10] C. K. Ho, R. Zhang, and Y.-C. Liang, “Two-Way Relaying over OFDM: Optimized Tone Permutation and Power Allocation,” in *IEEE International Conference on Communications (ICC’ 08)*. 2008, IEEE.

[11] K. Jitvanichphaibool, Rui Zhang, and Ying-Chang Liang, “Optimal Resource Allocation for Two-Way Relay-Assisted OFDMA,” in *IEEE Global Telecommunications Conference (GLOBECOM 2008)*, New Orleans, LO, USA, Nov. 2008.

[12] F. Li, G. Zhu, and D. Wang, “Optimal Power Allocation for Two-Way Relaying over OFDM using Physical-Layer Network Coding,” *The Journal of China Universities of Posts and Telecommunications*, vol. 18, no. 1, pp. 9–15, Feb. 2011.

[13] H. Shin and J. Lee, “Joint Resource Allocation for Multiuser Two-Way OFDMA Relay Networks with Proportional Fairness,” in *IEEE Vehicular Technology Conference (VTC Fall 2011)*, San Francisco, CA, USA, Sept. 2011.

[14] D. Wübben, M. Wu, and A. Dekorsy, “Physical-Layer Network Coding with Multiple-Antenna Relays,” in *MIMO Processing for 4G and Beyond: Fundamentals and Evolution*, Mario Marques da Silva; Francisco A. Monteiro, Ed. Apr 2014, CRC Press.

[15] I. W.-H. Ho, S.C. Liew, and L. Lu, “Feasibility Study of Physical-Layer Network Coding in 802.11p VANETs,” in *IEEE International Symposium on Information Theory (ISIT’ 14) 2014*, June 2014.

[16] M. Wu, F. Ludwig, M. Woltering, D. Wübben, A. Dekorsy, and S. Paul, “Analysis and Implementation for Physical-Layer Network Coding with Carrier Frequency Offset,” in *International ITG Workshop on Smart Antennas (WSA2014)*, Erlangen, Germany, Mar 2014.

[17] G. Wunder, P. Jung, M. Kasparick, T. Wild, F. Schaich, Y. Chen, S. ten Brink, I. Gaspar, N. Michailow, A. Festag, L. Mendes, N. Cassiau, D. Ktnas, M. Dryjanski, S. Pietrzyk, B. Eged, P. Vago, and F. Wiedmann, “5GNOW: Non-Orthogonal, Asynchronous Waveforms for Future Mobile Applications,” *Communications Magazine, IEEE*, vol. 52, no. 2, Feb. 2014.

[18] J. Du, *"Pulse Shape Adaptation and Channel Estimation in Generalised Frequency Division Multiplexing Systems"*, Licentiate Thesis in Electronics and Computer Systems, KTH, Stockholm, Sweden, Nov. 2008.

[19] W. Kozek and A.F. Molisch, “Nonorthogonal Pulseshapes for Multicarrier Communications in Doubly Dispersive Channels,” *IEEE Journal on Selected Areas in Communications*, vol. 16, no. 8, Oct 1998.

[20] G. Fettweis, M. Krondorf, and S. Bittner, “GFDM - Generalized Frequency Division Multiplexing,” in *IEEE 69th Vehicular Technology Conference, (VTC Spring 2009)*, Barcelona, Spain, April 2009.

[21] S. Schedler, M. Woltering, D. Wübben, V. Kühn, and A. Dekorsy, “Investigation on Gaussian Waveforms to Improve Robustness in Physical Layer Network Coding,” in *18th International OFDM Workshop 2014 (InOWo’14)*, Essen, Germany, Aug. 2014.

[22] X. Wang and V. H. Poor, “Iterative (Turbo) Soft Interference Cancellation and Decoding for coded CDMA,” *IEEE Transactions on Communications*, vol. 47, no. 7, pp. 1046–1061, 1999.

[23] M. Woltering, D. Wübben, A. Dekorsy, S. Schedler, and V. Kühn, “Physical Layer Network Coding Using Gaussian Waveforms: A Link Level Performance Analysis,” in *10th International ITG Conference on Systems, Communications and Coding (SCC’15)*, Hamburg, Germany, Feb 2015.

[24] L. Lu, T. Wang, S. C. Liew, and S. Zhang, “Implementation of Physical-Layer Network Coding,” *Physical Communication*, vol. 6, pp. 74–87, Mar. 2013.